Journal of Inorganic Biochemistry 198 (2019) 110749

Contents lists available at ScienceDirect

Journal of Inorganic Biochemistry

journal homepage: www.elsevier.com/locate/jinorgbio

DNA-binding and *in vitro* cytotoxic activity of platinum(II) complexes of curcumin and caffeine

Valentina Censi[a,b], Ana B. Caballero[a,c,*], Marta Pérez-Hernández[d], Vanessa Soto-Cerrato[d], Luís Korrodi-Gregório[d], Ricardo Pérez-Tomás[d], Maria Michela Dell'Anna[b], Piero Mastrorilli[b,**], Patrick Gamez[a,c,e,***]

[a] Department of Inorganic and Organic Chemistry, Inorganic Chemistry Section, University of Barcelona, Martí i Franquès 1-11, 08028 Barcelona, Spain
[b] DICATECh, Politecnico di Bari, via Orabona, 4, 70125 Bari, Italy
[c] Institute of Nanoscience and Nanotechnology (IN2UB), Universitat de Barcelona, Spain
[d] Department of Pathology and Experimental Therapeutics, Faculty of Medicine, University of Barcelona, Campus Bellvitge, Feixa Llarga s/n, 08907 L'Hospitalet de Llobregat, Spain
[e] Catalan Institution for Research and Advanced Studies (ICREA), Passeig Lluís Companys 23, 08010 Barcelona, Spain

ARTICLE INFO

Keywords:
Platinum(II) complex
Natural ligands
Caffeine
Curcumin
DNA interaction
Cytotoxicity
Photoactivation

ABSTRACT

Three Pt(II) complexes containing the natural ligands curcumin and caffeine, namely [Pt(curc)(PPh_3)$_2$]Cl (**1**), [PtCl(curc)(DMSO)] (**2**) (curc = deprotonated curcumin) and *trans*-[Pt(caffeine)Cl_2(DMSO)] (**3**), were synthesized and fully characterized. The data obtained suggest that, for both **1** and **2**, the anion of curcumin is coordinated to the platinum ion *via* the oxygen atoms of the β-diketonate moiety. Spectroscopic features reveal that in **2** and **3**, a DMSO molecule is S-bonded to the metal centre. For **3**, all data indicate a square-planar geometry formed by a 9-N bonded caffeine, two *trans* chloride anions and a DMSO. The three complexes undergo changes in solution upon incubation for 24 h; **1** and **2** release curcumin while **3** isomerizes from *trans* to *cis* configuration. The DNA-binding and cytotoxic properties of **1**–**3** were evaluated *in vitro*. Despite their structural similarity, curcuminate-containing **1** and **2** exhibit distinct DNA interactions. While **1** appears to intercalate between nucleobase pairs, inducing the oxidative degradation of the biomolecule, **2** behaves as a groove binder, by means of electrostatic forces. Caffeine-containing **3** exhibits a behaviour that is comparable to that of **2**. Complexes **1** and **2** showed moderate to high cytotoxicity and selectivity against several cancer cell lines, while **3** is inactive. Compounds **1** and **2** can be further activated by visible-light irradiation.

1. Introduction

The International Agency for Research on Cancer (IARC) estimated that 14.1 million new cancer cases and 8.2 million cancer deaths (which correspond to about 22,000 cancer deaths a day) occurred in 2012 [1]. These figures are expected to grow significantly, so that 21.7 million new cancer cases and 13 million cancer deaths will be witnessed by 2030 [2]. Thus, cancer is a major public health problem worldwide and investigation is definitively required to develop new efficient drugs [3–6].

Cisplatin [7] is one of the most used anticancer agents worldwide [8]. However, it exhibits several drawbacks, *e.g.* its use is limited to a restricted number of cancers [9], acquired or intrinsic cisplatin resistance may be shown by some tumors [10], and it causes severe side effects, such as nausea, nephrotoxicity, ototoxicity or myelosuppression [11,12]. Therefore, the design of new platinum-based compounds is a hot topic of current research in the field; actually, a number of platinum drugs have been developed and marketed, *viz.* the second-generation platinum chemotherapy agents carboplatin and nedaplatin, and the third-generation complexes oxaliplatin and lobaplatin [13–16].

Naturally occurring ligands, especially those approved by the Food and Drug Administration (FDA) for diverse applications, represent molecules of choice for the preparation of metal-based compounds, as they may accelerate the procedure to reach marketing approval for an

* Correspondence to: A. B. Caballero, Department of Inorganic and Organic Chemistry, Inorganic Chemistry Section, University of Barcelona, Martí i Franquès 1-11, 08028 Barcelona, Spain.
** Corresponding author.
*** Correspondence to: P. Gamez, Catalan Institution for Research and Advanced Studies (ICREA), Passeig Lluís Companys 23, 08010 Barcelona, Spain.
E-mail addresses: ana.caballero@ub.edu (A.B. Caballero), pietro.mastrorilli@poliba.it (P. Mastrorilli), patrick.gamez@qi.ub.es (P. Gamez).

https://doi.org/10.1016/j.jinorgbio.2019.110749
Received 12 February 2019; Received in revised form 3 June 2019; Accepted 5 June 2019
Available online 07 June 2019

active compound. In this context, a number of metal complexes based on natural ligands have been described in the literature; for example, coordination compounds from curcumin (1,7-bis-(4-hydroxy-3-methoxyphenyl)-1,6-heptadiene-3,5-dione) have been reported for medicinal applications [17,18]. Caffeine-derived complexes of rhodium (I) or gold(I) have shown promising anticancer properties [19].

In fact, curcumin displays a wide therapeutic profile as it has been reported for its antioxidative, anti-inflammatory, antiviral, antibacterial, antifungal, and anticancer properties [20–22]. However, curcumin possesses serious disadvantages that hinder its use as a therapeutic agent: low aqueous solubility, rapid metabolism leading to degradation, and reduced bioavailability [23]. Caffeine, apart from its known anti-inflammatory activity, modulates the antitumor activity of several drugs; it is thought to increase the antitumor effect of cisplatin or DNA-damaging agents by inhibiting DNA repair [24–26].

In the search for new platinum-based anticancer therapeutics, DNA is still the first selected target to test the therapeutic potential of newly synthesized compounds. This is because of the structural resemblance of Pt(II) complexes with its well-known, DNA-targeted predecessors cisplatin and oxaliplatin, which are DNA binders producing unrepairable damages to the biomolecule that lead to cell death.

In the present study, curcumin and caffeine have been selected as natural and bioactive building-blocks to obtain three new platinum(II) complexes with *in vitro* antiproliferative activity against some cancer cell lines. Reports have shown that the coordination of these bioactive molecules to d [25–27]- and f-block metal ions can greatly improve their aqueous solubility, bioavailability, and antitumor activity [25,27,28]. Hence, the complexes [Pt(curc)(PPh_3)$_2$]Cl (**1**) and [PtCl(curc)(DMSO)] (**2**) (curc = deprotonated curcumin), in which the anion of curcumin should act as a leaving group once the complexes enter the cells, and *trans*-[Pt(caffeine)Cl_2(DMSO)] (**3**) were prepared and fully characterized. As carrier ligands we used triphenylphosphane (PPh_3) and dimethylsulfoxide (DMSO); PPh_3 may enhance the diffusion through cell membranes and DMSO should improve the complex solubility in water.

The changes taking place upon incubation of the complexes in solution are discussed and related to their DNA-binding features and cytotoxicity. Cytotoxicity assays against several cancer cell lines and a non-tumorigenic one, reveal the great therapeutic potential of curcuminate complexes **1** and especially **2**, which displayed half-maximal inhibitory concentrations (IC_{50}) in the range of 6–23 μM. The cytotoxic effect of [PtCl(curc)(DMSO)] (**2**) clearly surpassed those of its parent drug cisplatin and free curcumin. Moreover, the photosensitizing nature of curcumin exerted an even higher cytotoxicity to this complex, reaching IC_{50} values as low as 2.5 μM upon irradiation with visible light for 1 h.

2. Experimental

2.1. Materials and instrumentation

cis-$PtCl_2(PPh_3)_2$ [29] and K[$PtCl_3$(DMSO)] [30] were synthetized according to literature methods. IR spectra were recorded on a Bruker-Vector 22 spectrometer. NMR spectra were recorded on a Bruker Advance 400 spectrometer Bruker Advance 400 spectrometer or on a Bruker Avance III 700 MHz instrument equipped with cryoprobe; chemical shifts are in ppm and coupling constants in Hz; the frequencies are referred to Me_4Si for ^1H (400 MHz) and for ^{13}C (100 MHz), to 85% H_3PO_4 for ^{31}P (121.5 MHz) and to H_2PtCl_6 for ^{195}Pt (85.99 MHz) NMR. Elemental analyses were obtained on a EuroVector CHNS EA3000 elemental analyser using acetanilide as analytical standard material. Triplicate analysis runs have been performed to ensure reproducibility. High-resolution mass spectrometry (HR-MS) analyses were performed using a time-of-flight mass spectrometer equipped with an electrospray ion source (Bruker micrOTOF). The calculated (exact mass) and the experimental (accurate) *m/z* values were compared considering the isotope pattern of the main ion (that is giving the most intense peak), by using the software Bruker Daltonics Data Analysis (version 3.3). The melting points were determined with a Büchi Melting Point B-540 apparatus and are uncorrected. Caffeine was purchased from Alpha Aesar, potassium tetrachloroplatinate(II) was purchased from ChemPur, curcumin, PPh_3 and the sodium salt of calf thymus DNA (ct-DNA, Type I fibrous) were purchased from Sigma-Aldrich. Plasmid pBR322 DNA (4361 bp, 0.25 mg mL^{-1}) was obtained from Thermo Scientific. Ethidium bromide (EB) 10 mg mL^{-1} solution and tris(hydroxymethyl)aminomethane (Tris base) were purchased from Promega. Agarose (D-1, Low EEO) was purchased from Pronadisa. N-(2-hydroxyethyl)piperazine-N′-(2-ethanesulfonic acid) (HEPES) and (3-(4,5-dimethylthiazol-2-yl)-2,5-diphenyl-tetrazolium bromide (MTT) were obtained from Sigma-Aldrich. All reagents were of molecular biology grade and used without further purification.

2.2. Synthesis of [Pt(curc)(PPh_3)$_2$]Cl (1)

A solution of KOH (1.46 mmol, 0.0853 g) in ethanol (4.0 mL) at 40 °C was added dropwise to an orange solution obtained by dissolving curcumin (1.46 mmol, 0.5408 g) and *cis*-$PtCl_2(PPh_3)_2$ (0.725 mmol, 0.5766 g) in 40 mL of CH_2Cl_2 at room temperature. The resulting dark-red mixture was stirred at room temperature overnight. Then, the reaction mixture was filtered to remove KCl and dried under high vacuum. The resulting brown oleum was recrystallized from CH_2Cl_2/Et_2O and the dark-green solid obtained was filtered off and washed with ethanol and diethyl ether, and subsequently dried under high vacuum. Yield: 0.695 g, 85%. M.p. = 200.1 °C. Anal. Calcd. for $C_{57}H_{49}ClO_6P_2Pt$ [Mw: 1122.49]: C, 60.99; H, 4.40. Found: C, 61.17; H, 4.45.

HRMS (ESI, acetonitrile, positive ion mode) *m/z*: calcd. for $C_{57}H_{49}O_6P_2Pt$ [M-Cl]$^+$ 1086.2643; found. 1086.2651.

^1H NMR (400 MHz, DMSO-d_6, 298 K) δ, ppm: 7.53 (m, 6H, H_{para}, PPh_3), 7.52 (m, 12H, H_{meta}, PPh_3), 7.38 (m, 12H, H_{ortho}, PPh_3), 7.27 (s, 2H, H^{10}), 7.11 (d, 2H, H^6, $^3J_{HH}$ = 8.0 Hz), 6.79 (d, 2H, H^7, $^3J_{HH}$ = 8.0 Hz), 6.45 (d, 2H, H^3, $^3J_{HH}$ = 15.0 Hz), 5.97 (s, 1H, H^1), 5.79 (d, 2H, H^4, $^3J_{HH}$ = 15.0 Hz), 3.81 (s, H^6, –OCH_3). $^{13}C\{^1H\}$ [31] NMR (100 MHz DMSO-d_6, 298 K) δ, ppm: 175.0 (C^2), 148.9 (C^8), 148.8 (C^9), 141.2 (C^4), 134.7 (C_{meta}, PPh_3), 132.4 (C_{para}, PPh_3), 129.2 (C_{ortho}, PPh_3), 126.8 (C_{ipso}, PPh_3), 126.4 (C^5), 124.1 (C^3), 123.7 (C^6), 116.4 (C^7), 111.7 (C^{10}), 105.1 (C^1), 56.0 (OCH_3). $^{31}P\{^1H\}$ NMR (121.5 MHz, DMSO-d_6, 298 K) δ, ppm: 8.6 (s, $^1J_{Pt,P}$ = 3876 Hz). $^{195}Pt\{^1H\}$ NMR (85.99 MHz, DMSO-d_6, 298 K) δ, ppm: −3951 (t, $^1J_{Pt,P}$ = 3876 Hz).

IR (KBr, cm^{-1}): 3496 (b, m, $\nu_{O\text{-}H}$), 1971–1813 (w, aromatic overtones), 1620 (s, $\nu_{C=O}$ + $\nu_{C=C}$), 1601 (s, $\nu_{C=C}$ + $\nu_{C=O}$), 1511 (s, $\nu_{C=C}$), 1292 (m, δ_{C-O-C}), 1266 (m, ν_{C-O}), 1158 (m, ν_{O-H}).

2.3. Synthesis of [PtCl(curc)(DMSO)] (2)

0.0686 g (0.164 mmol) of K[$PtCl_3$(DMSO)] was dissolved in 5 mL of water. A solution of an equimolar amount of curcumin (0.0710 g, 0.1604 mmol) and KOH (9.00 mg, 0.1604 mmol) in ethanol (2.5 mL) was added dropwise to the K[$PtCl_3$(DMSO)] solution, resulting in an immediate darkening of the resulting mixture. The mixture was left under vigorous stirring at room temperature for 36 h. Then, it was kept at 277 K overnight, giving rise to the precipitation of a brown solid, which was filtered off, washed with ethanol and diethyl ether, and dried under high vacuum. Yield: 0.0786 g, 71%. M.p. = 142.4 °C. Anal. calcd. for $C_{23}H_{25}ClO_7PtS$ [Mw: 676.04]: C, 40.88; H, 3.73. Found: C, 40.50; H, 3.47.

HRMS (ESI, acetonitrile, positive ion mode) *m/z*: calcd. for $C_{23}H_{25}ClO_7PtSNa$ [M + Na]$^+$ 699.0550; found. 699.0538.

IR (nujol mull, cm^{-1}): 3378 (b, m, $\nu_{O\text{-}H}$), 1623 (s, $\nu_{C=O}$ + $\nu_{C=C}$), 1590 (s, $\nu_{C=C}$ + $\nu_{C=O}$), 1511 (s, $\nu_{C=C}$), 1268 (m, ν_{C-O}), 1123 (s, $\nu_{S=O}$), 296 (m, ν_{Pt-Cl}).

^1H NMR (700 MHz $CDCl_3$, 298 K) δ, ppm: 7.70 (d, 1H, H^4, $^3J_{H,H}$ = 15.6 Hz), 7.56 (d, 1H, $H^{4'}$, $^3J_{HH}$ = 15.6 Hz), 7.16 (d, 1H, H^6,

$^{3}J_{HH}$ = 8 Hz), 7.14 (d, 1H, H$^{6'}$, $^{3}J_{HH}$ = 8 Hz), 7.04 (broad s, 1H, H^{10}), 7.03 (broad s, 1H, H$^{10'}$), 6.92 (d, 1H, H^{7}, $^{3}J_{HH}$ = 8 Hz), 6.91 (d, 1H, H$^{7'}$, $^{3}J_{HH}$ = 8 Hz), 6.51 (d, 1H, H^{3}, $^{3}J_{HH}$ = 15.6 Hz), 6.48 (d, 1H, H$^{3'}$, $^{3}J_{HH}$ = 15.6 Hz), 5.83 (s, 1H, H^{1}), 3.94 (s, 3H, –OCH_3), 3.93 (s, 3H, –OCH_3'), 3.57 (-CH_3, 6H, coordinated DMSO). ^{13}C{^{1}H} NMR (176 MHz $CDCl_3$, 298 K) d, ppm: 176.2 (C^{2}), 176.0 (C$^{2'}$), 147.7 (C$^{8,8'}$), 146.6 (C$^{9,9'}$), 142.0 (C^{4}), 141.1 (C$^{4'}$), 127.8 (C^{5}), 127.6 (C$^{5'}$), 122.4 (C^{6}), 122.8 (C$^{6'}$), 122.1 (C^{3}), 121.8 (C$^{3'}$), 114.8 (C^{7}), 115.0 (C$^{7'}$), 110.0 (C^{10}), 109.5 (C$^{10'}$), 103.9 (C^{1}), 55.9(–OCH_3), 44.8 (–CH_3, coordinated DMSO). ^{195}Pt {^{1}H} NMR (86 MHz $CDCl_3$, 298 K) δ, ppm: −2381 (s).

2.4. Synthesis of trans-[Pt(caffeine)Cl_2(DMSO)] (3)

A solution containing 0.1276 g (0.657 mmol) of caffeine in 9 mL of water was added dropwise to a solution obtained by dissolving 0.2503 g (0.597 mmol) of K[$PtCl_3$(DMSO)] in 5 mL of water. The addition of the first drops of caffeine solution caused a colour change of the platinum-containing solution, from orange to peach pink, with concomitant precipitation of a white solid. The mixture was left under vigorous stirring at room temperature for 12 h. Then, the white solid was removed by filtration from the reaction mixture, washed with ethyl alcohol and diethyl ether, and dried under high vacuum. Yield: 0.1786 g, 58%. M.p. = 232.4 °C. The complex is soluble in DMSO and slightly soluble in $CHCl_3$. Anal. calcd. for $C_{10}H_{16}Cl_2N_4O_3PtS$ [Mw: 538.31 Da]: N, 10.41; C, 22.31; H, 3.00. Found: N, 10.34; C, 22.36; H, 2.79. ^{1}H NMR (400 MHz $CDCl_3$, 298 K) δ, ppm: 7.94 (q, H^{1}, 8-H, $^{4}J_{HH}$ = 0.7 Hz), 4.40 (s, 3H, H^{3}), 4.12 (d, 3H, H^{7}, $^{4}J_{HH}$ = 0.7 Hz), 3.52 (s, 6H, –CH_3 of DMSO group), 3.44 (s, 3H, H^{1}). ^{13}C{^{1}H} NMR (101 MHz $CDCl_3$, 298 K) δ, ppm: 154.3 (C^{6}), 151.0 (C^{2}), 145.1 (C^{4}), 140.7 (C^{8}), 108.4 (C^{5}), 44.2 (–CH_3 of DMSO), 35.1 (C^{7}), 33.4 (C^{3}), 28.5 (C^{1}). ^{195}Pt{^{1}H} NMR (85.99 MHz, $CDCl_3$, 298 K) δ, ppm: −3009 (s).

IR (nujol mull, cm^{-1}): 1716 (s, $\nu_{C=O}$), 1668 (s, $\nu_{C=O}$), 1612 (w, $\nu_{C=N}$), 1240 (m, ν_{C-N}), 1145 (s, $\nu_{S=O}$), 341 (m, ν_{Pt-Cl}).

HRMS (ESI, methanol, positive ion mode) *m/z*: calcd. for $C_{10}H_{16}Cl_2N_4O_3PtSNa$ [M + Na]$^{+}$ 560.9857, found. 560.9834; calcd. for $C_{10}H_{16}Cl_2N_4O_3PtSK$ [M + K]$^{+}$ 576.9596, found 576.9577; calcd. for $C_{20}H_{32}Cl_4N_8O_6Pt_2S_2Na$ [2 M + Na]$^{+}$ 1098.9790, found 1098.9798.

2.5. UV–vis measurements

Electronic spectra were recorded on a Varian Cary 100 Scan spectrophotometer at room temperature employing a 1.0 cm path length cuvette. Stock solutions of complexes **1–3** were prepared in DMSO. For the stability studies, UV–Vis spectra of 25 μM solutions of **1–3** in PBS (containing 1% DMSO) were recorded over a period of 24 h. For the DNA-binding assays, the concentration of ct-DNA was determined from the absorption intensity at 260 nm and the corresponding molar absorptivity of 6600 M^{-1} cm^{-1} (nucleobase concentration). Absorption titration experiments were carried out by adding increasing amounts of ct-DNA (0–50 μM) to a 25 μM solution of the compound in cacodylate-NaCl buffer (1.0 mM sodium cacodylate, 20 mM NaCl, pH 7.2). The final concentration of DMSO was 0.25%. The spectra were recorded after equilibration for 5 min at 20 °C. Corrections were made for the absorbance of ct-DNA itself.

The intrinsic binding constant (K_b) was determined from the titration data using Eq. (1):

$$\frac{[DNA]}{\varepsilon_a - \varepsilon_f} = \frac{[DNA]}{\varepsilon_0 - \varepsilon_f} + \frac{1}{K_b(\varepsilon_0 - \varepsilon_f)} \quad (1)$$

where ε_a, ε_0, and ε_f are respectively, the molar extinction coefficients of the free complexes in solution, fully bound complex with DNA, and complex bound to DNA at a definite concentration.

2.6. Fluorescence measurements

Emission intensity of the DNA-intercalator ethidium bromide (EB) was measured using an iHR320 HORIBA JOBIN YVON spectrofluorometer. The samples contained 15 μM (base pairs) of ct-DNA and 75 μM EB in 1.0 mM cacodylate – 20 mM NaCl buffer (pH 7.2). In a first instance, EB was incubated with ct-DNA for 30 min, to allow the intercalation of EB between DNA base pairs. Afterwards, increasing amounts of compounds **1–3** (0–25 μM) were added and the final samples were incubated for 24 h. A maximum of 5% DMSO was used to solubilise the complexes. The fluorescence spectra of all complexes were recorded at room temperature, at λexc = 514 nm.

For the displacement assays of the minor-groove binder Hoechst 33258, 0.10 mM of the dye was used and the same conditions as those used for the EB-displacement assays were applied. The fluorescence spectra were recorded at λexc = 350 nm.

2.7. Agarose gel electrophoresis

Stock solutions of the platinum(II) compounds were prepared in 1.0 mM cacodylate – 20 mM NaCl buffer (pH = 7.2) containing 2% DMSO. pBR322 plasmid DNA aliquots (50 μM base pairs) in 1 mM cacodylate – 20 mM NaCl buffer were incubated with the complexes for 24 h at 37 °C. Next, the reaction samples were quenched with 4 μL of loading buffer (5 mM xylene cyanol and 30% glycerol) and electrophoresed on 1% agarose gel in 1× Tris-Borate-EDTA buffer (89 mM Tris pH 7.6, 89 mM boric acid and 2 mM EDTA) for 90 min at 6.5 V cm^{-1}. The electrophoresis was run in a BioRad horizontal tank connected to a CONSORT EV231 electrophoresis power supply. Free DNA was used as control. Afterwards, the DNA was stained with SYBR® Safe overnight and the gel was photographed with a BioRad Gel Doc EZ Imager.

2.8. Circular dichroism (CD) spectroscopy

Circular dichroism (CD) spectra were recorded using a JASCO-815 spectropolarimeter, equipped with a xenon-arc lamp of 450 W, and connected to a computer to carry out the data processing. The sample compartment was air-purged with N_2 before use. For the measurements, quartz cuvettes with an optical path of 5 mm were used. The concentration of ct-DNA was determined from its absorption intensity at 260 nm, with a molar extinction coefficient of 6600 M^{-1} cm^{-1}. A solution of 200 μM ct-DNA in 1.0 mM cacodylate – 20 mM NaCl buffer (pH 7.2) was incubated for 24 h with metal complex/DNA ratios of 0–1 (except for compound **1**, which precipitated at ratios over 0.2 at 37 °C) before recording the CD spectra at room temperature.

2.9. Atomic force microscopy (AFM)

pBR322 plasmid DNA aliquots (0.2 mg mL^{-1}) in 40 mM HEPES – 10 mM $MgCl_2$ buffer were incubated with the complexes for 24 h at 37 °C. The AFM samples were prepared by casting a 5 μL drop of test solution onto freshly cleaved muscovite green mica disks as the support. The drop was allowed to stand for 3 min to favour the adsorbate–substrate interaction. Each DNA laden disk was rinsed with Milli-Q water and was blown dry with clean compressed argon gas directed normal to the disk surface. The samples were stored over silica prior to AFM imaging. Images were recorded with a Bruker AFM Multimode8 with nanoscope V electronics using a SNL tip and Scan Asyst mode (1 Hz).

2.10. Cell culture and cell-viability assays

Human melanoma A375, lung A549, breast MCF-7, ovary SKOV3 colorectal SW620 adenocarcinoma and non-tumorigenic epithelial breast MCF10A cell lines were obtained from the American Type Culture Collection (ATCC, Manassas, VA, USA). The cell lines A549,

A375, SKOV3 and SW620 were cultured in DMEM medium with 10% heat-inactivated fetal bovine serum (FBS; Life Technologies, Carlsbad, CA, USA), 100 U mL^{-1} penicillin, 100 μg mL^{-1} streptomycin, and 2.0 mM glutamine. The MCF-7 cell line was cultured in DMEM–F12 (HAM) media (1:1) with 10% FBS, 50 μM sodium pyruvate (Sigma-Aldrich Chemical Co., St. Louis, MO, USA), 10 μg mL^{-1} insulin (Sigma-Aldrich), 100 U mL^{-1} penicillin, 100 μg mL^{-1} streptomycin, and 2 mM glutamine. MCF10A cells were cultured in DMEM–F12 (HAM) media (1:1) with 5% horse serum (Life Technologies), 100 U mL^{-1} penicillin, 100 μg mL^{-1} streptomycin, 2.0 mM glutamine, 10 μg mL^{-1} insulin 0.5 μg mL^{-1} hydrocortisone (Sigma-Aldrich), 20 ng mL^{-1} epidermal growth factor (EGF, Sigma-Aldrich), 100 ng mL^{-1} choleric toxin (Calbiochem, San Diego, CA, USA). Both the media and the added chemicals whenever not stated were obtained from the Biological Industries, Beit Haemek, Israel. Cells were grown at 37 °C in a 5% CO_2 atmosphere.

10^4 cells were seeded in 96-well plates (10^5 cells mL^{-1}) and allowed to grow for 24 h. For single-point experiments, the cells reacted with the investigated compounds at two different concentrations (10 μM and 50 μM) and incubated for 24 h. For the dose–response curves, the cells were treated with different concentrations of the compounds (from stock solutions in DMSO), in the range of 0.16–20 μM for compound **1** and cisplatin dissolved in PBS or in the range of 0.78–100 μM for compound **2**, curcumin and cisplatin dissolved in DMSO, and incubated for 24 h. Prior to cell treatment, the compounds were freshly dissolved (referred as Fresh in Table 1) or incubated in the corresponding culture medium for 24 h at 37 °C (referred as Pre-incubated). After dosing the compounds, the cells were incubated 1 h at room temperature in the dark (Non-irradiated) or under visible light (Irradiated). These steps were followed by 24 h incubation at 37 °C. Next, a 10 μM solution of MTT (3-(4,5-dimethylthiazol-2-yl)-2,5-diphenyl-tetrazolium bromide) was added to each well and the plates were incubated at 37 °C for two additional hours. The medium was removed, and the purple formazan crystals were dissolved in 100 μL of DMSO. The absorbance was measured at 570 nm using a multi-well plate reader (Multiskan FC, Thermo Scientific). The cell viability was calculated according to the relation: viability (%) = [(absorbance of the treated wells) / (absorbance of the control wells)] × 100.

The IC_{50} values (corresponding to the compound concentrations that produce 50% reduction in cell viability) were obtained from the dose–response curves using GraphPad Prism V5.0 for Windows™ (GraphPad Software, San Diego, CA, USA). All data are shown as the mean value ± S.D. of three independent experiments for single-point assays and for the dose–response curves.

3. Results and discussion

3.1. Synthesis and characterization of compounds 1–3

Deprotonated curcumin binds almost all metals due to its β-diketonate moiety, which is known to be an excellent chelating group, owing to the delocalization of the π electrons in the resulting ring and the consequent stabilization of the overall system [32]. In addition, the coordination of curcumin to a metal centre protects curcumin itself against homo-polymerization and photo-degradation, and modifies its solubility in some solvents, depending on the nature of the other ligands bound to the metal centre. In fact, the major problems associated to the use of the sole curcumin as a drug arise from its poor solubility in water under physiological conditions, enhanced by its tendency to polymerize, and its low stability to sunlight. Thus, the binding of curcumin to a metal could increase its biological features, as it has been observed for $[Pt(curc)(NH_3)_2]NO_3$ (curc = deprotonated curcumin) [28], which is a cisplatin analogue, showing synergic anticancer effects between a platinum-based drug and curcumin. Recently, triarylphosphane-bearing platinum complexes have been revaluated from a cytotoxic point of view [33], due to their ability to across the cell membrane, thanks to lipophilic phosphane groups [34]. Triphenylphosphane platinum complexes carrying the deprotonated form of biologically active flavonoids showed interesting cytotoxic activity against selected cell lines [35]. Following our studies on platinum complexes with naturally occurring biologically active ligands, we decided to synthetize curcumin-containing Pt complexes bearing triphenylphosphane or dimethyl sulfoxide (DMSO) as carrier ligands.

Curcumin exhibits a tautomeric equilibrium with two possible structures through intramolecular hydrogen transfer. The typical predominance of the enol form in solution facilitates the α-deprotonation under alkaline conditions and promotes the *O,O′*-bidentate coordination to a metal centre. In fact, we easily obtained $[Pt(curc)(PPh_3)_2]Cl$ (**1**) by reaction of curcumin with *cis*-$[PtCl_2(PPh_3)_2]$ in the presence of an equimolar amount of KOH with respect to curcumin (Scheme 1).

The HR ESI-MS(+) spectrogram of a diluted acetonitrile solution of **1** shows an intense peak at *m/z* 1086.2643, whose isotope pattern is perfectly superimposable to that calculated for the cation $[Pt(curc)(PPh_3)_2]^+$.

The $^{31}P\{^1H\}$ NMR spectrum of **1** in DMSO-d_6 exhibits a singlet at δ 8.6 ppm flanked by satellites from which a $^1J_{PtP}$ value of 3876 Hz could be extracted. The $^{195}Pt\{^1H\}$ NMR spectrum shows a triplet at δ −4400 ppm. These data are consistent with a Pt(II) phosphane complex [36], bearing two magnetically equivalent ^{31}P nuclei mutually in *cis* positions [37], and in *trans* position with respect to an anionic dioxygen

Table 1
IC_{50} values obtained with cisplatin (stock solution prepared in PBS), free curcumin, and complex **2**, against MCF-7 (breast adenocarcinoma), MCF-10A (non-tumorigenic epithelial breast cell line) and SW620 (colorectal adenocarcinoma) cells, after incubation for 24 h at 37 °C. Freshly prepared or pre-incubated (for 24 h) solutions of the compounds in the culture medium were evaluated. Once the compounds were added, the cells were incubated for 1 h at room temperature in the dark or under visible-light irradiation, and for further 23 h at 37 °C. The results are means ± SD of four independent experiments.

			IC_{50} (μM)		
			MCF7	SW620	MCF10A
Cisplatin (PBS)	Freshly prepared	Non-irradiated	28.3 ± 2.2	17.2 ± 8.8	12.0 ± 0.8
		Irradiated	26.2 ± 1.0	23.1 ± 0.5	13.1 ± 0.2
	Pre-incubated 24 h	Non-irradiated	> 20	> 20	> 20
		Irradiated	> 20	> 20	> 20
Curcumin	Freshly prepared	Non-irradiated	40.5 ± 10.2	15.5 ± 2.9	37.4 ± 18.9
		Irradiated	5.6 ± 1.4	10.8 ± 3.4	5.9 ± 1.7
	Pre-incubated 24 h	Non-irradiated	> 100	85.6 ± 4.6	> 100
		Irradiated	36.4 ± 12.2	51.1 ± 6.3	60.2 ± 22.5
Compound **2**	Freshly prepared	Non-irradiated	11.6 ± 5.0	6.1 ± 1.8	22.9 ± 9.9
		Irradiated	2.5 ± 0.3	4.1 ± 1.0	4.3 ± 1.9
	Pre-incubated 24 h	Non-irradiated	66.1 ± 12.9	83.0 ± 15.6	85.2 ± 23.8
		Irradiated	19.5 ± 6.8	36.5 ± 3.3	31.5 ± 11.9

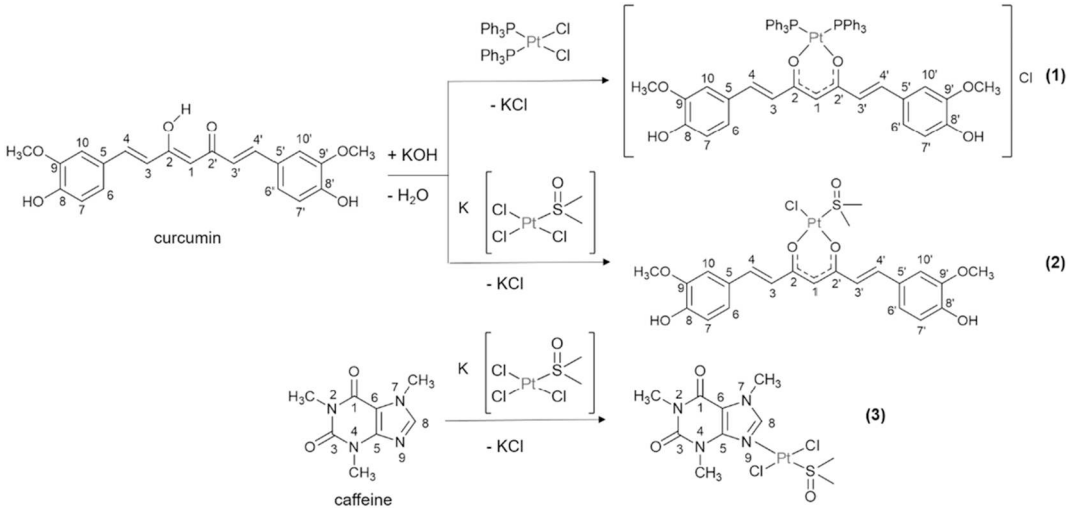

Scheme 1. Synthetic pathways for the preparation of compounds **1–3**. (For interpretation of the references to colour in this figure, the reader is referred to the web version of this article.)

ligand [33,35]. Accordingly, in the ^{1}H NMR spectrum, the signal of the intramolecular hydrogen bonded enolic proton, which falls at δ 10.05 ppm for the free ligand [38], is not observed and the γ-proton signal of the coordinated diketone moiety (δ 5.97 ppm) is shifted 0.08 ppm up-field with respect to that of free curcumin (δ 6.15 ppm), as it occurs for similar curcumin-chelated metal complexes [39,40]. Analogously, the ^{13}C{^{1}H} NMR spectrum of **1** in DMSO-d_6 reveals a 7 ppm up-field shift of the magnetically equivalent β-diketonate ^{13}C carbonyl signal (δ 176.0 ppm) with respect to the carbonyl peak of free curcumin (δ 183.6 ppm), as it has been found in the ^{13}C{^{1}H} NMR spectrum of [Pt(curc)$(NH_3)_2$]NO_3 [28], whose structure is very similar to that proposed for complex **1**. In addition, the ^{13}C and ^{1}H NMR data evidence only one set of signals for **1**, indicating a symmetric molecule, thus corroborating a chelate curcumin coordination. The other NMR spectroscopic features were unequivocally assigned by 2D NMR experiments and are reported in the Experimental section.

The IR spectrum of **1** shows the two characteristic bands at 1620 cm^{-1} and 1601 cm^{-1}, [39,41] assigned to $\nu_{C=O}$ coupled with $\nu_{C=C}$ and to $\nu_{C=C}$ coupled with $\nu_{C=O}$, respectively, which are typical for metal chelate β-diketonate systems [39,40] [42]. No Pt−Cl stretching peak was detected in the far IR region for complex **1**, suggesting that metal coordination by chloride [43] did not occur, as already observed in similar platinum(II) complexes [35].

Some Pt(II) and Pd(II) complexes containing β-diketonate ligands and DMSO have been recently synthetized, the platinum ones displaying higher cytotoxicity against selected cancer cells than the free ligands [44]. Inspired by these findings, we decided to synthesize a platinum compound bearing anionic curcumin, as leaving group, and DMSO, as carrier ligand, exploiting the procedure already successfully used for the synthesis of some β-diketonate Pt complexes containing DMSO as ligand [45]. Thus, the reaction of K[PtCl$_3$(DMSO)] with deprotonated curcumin (Scheme 1) gave in high yield complex [PtCl(curc)(DMSO)] (**2**). To prevent metal reduction, a slight excess of curcumin was used with respect to the 1:1 ratio of KOH/platinum precursor [45].

The results of the elemental analyses (see Experimental section) and of the HRMS measurements (Fig. S1) are in accordance with the proposed structure.

The IR spectrum of **2** shows typical bands for chelate curcumin complexes, namely at 1623 cm^{-1} ($\nu_{C=O}$ + $\nu_{C=C}$) and 1590 cm^{-1} ($\nu_{C=C}$ + $\nu_{C=O}$), along with a strong absorption at 1511 cm^{-1} ascribed to $\nu_{C=C}$. The presence of an intense S=O stretching band at 1123 cm^{-1} indicates that DMSO is coordinated to platinum through its sulfur atom [42]. The Pt−Cl stretching band appears at 296 cm^{-1}. In the ^{1}H NMR spectrum, the expected differentiation between the two halves of the coordinated curcumin was observed. For instance, the signals of H^3 and H$^{3'}$ were found at δ 6.51 and δ 6.48, respectively, while the signals of H^4 and H$^{4'}$ were found at δ 7.70 and δ 7.56, respectively. The ^{195}Pt{^{1}H} signal was found at δ −2381, a value comparable to that observed for the related complex [PtCl(acac)(DMSO)] (δ_{Pt} − 2399). [32]

As mentioned above, **1** and **2** contain the biologically active ligand (*i.e.* the curcuminate) as *leaving group*. Next, a Pt complex bearing a biologically active molecule as *carrier* ligand was designed and prepared, namely *trans*-[Pt(caffeine)Cl$_2$(DMSO)] (**3**). Caffeine is a purine-type alkaloid that is well-known for its anticancer effects [46]. The caffeine complex **3** was synthesized modifying a reported procedure used for the synthesis of *trans*-[PtCl$_2$(DMSO)(py)] (py = pyridine) [30], *i.e.* by reaction between K[PtCl$_3$(DMSO)] and a slight excess of caffeine.

The HR ESI-MS data achieved for **3** in methanol showed an intense peak at *m/z* 560.9834, ascribed to the sodium adduct [**3** + Na]$^+$ along with peaks at *m/z* 576.9577 ([**3** + K]$^+$) and at *m/z* 1098.9798 (attributed to the sodium adduct of a dimer of **3**).

The IR spectrum showed, beside the Pt−Cl stretching band at 341 cm^{-1}, two bands at 1716 cm^{-1} and 1668 cm^{-1}, ascribed to C=O stretching vibrations. The $\nu_{C=O}$ values for free caffeine are 1702 cm^{-1} and 1662 cm^{-1}, hence indicating that the C=O groups are not coordinated to the metal [47]. The presence of a strong band at 1145 cm^{-1} assigned to the S=O stretching indicates that DMSO is S-coordinated to platinum [39].

The ^{1}H NMR spectrum of complex **3** in $CDCl_3$ showed the signal attributable to H^8 at δ 7.94 ppm, typical for Pt coordination of caffeine through the nitrogen atom N^9 [48]. In addition, the ^{1}H-^{195}Pt HMQC spectrum of **3** in $CDCl_3$ (Fig. 1) clearly revealed couplings between the ^{195}Pt nucleus and: *H*^{8} (δ 7.94), N^3-*CH*$_3$ (δ 4.40), and the coordinated DMSO (δ 3.52 ppm), whose CH_3 protons at δ 3.52 ppm are typical for an S-bonded ligand [49].

The ^{195}Pt NMR signal in $CDCl_3$ was found at δ −3009, which is consistent with *trans*, square-planar Pt(II) dichloride complexes containing DMSO and N-bonded heterocycles [50]. The ^{13}C{^{1}H} NMR spectrum of **3** showed signals for the coordinated caffeine which were slightly de-shielded with respect to those of free caffeine [51].

3.2. Stability of complexes 1–3

The behaviour/stability of compounds **1–3** in solution was first evaluated by UV–Vis spectroscopy, in PBS containing 1% DMSO at 37 °C. UV–Vis spectra solutions of the different compounds were thus recorded during 24 h. As observed in Fig. S2, the curcumin-based

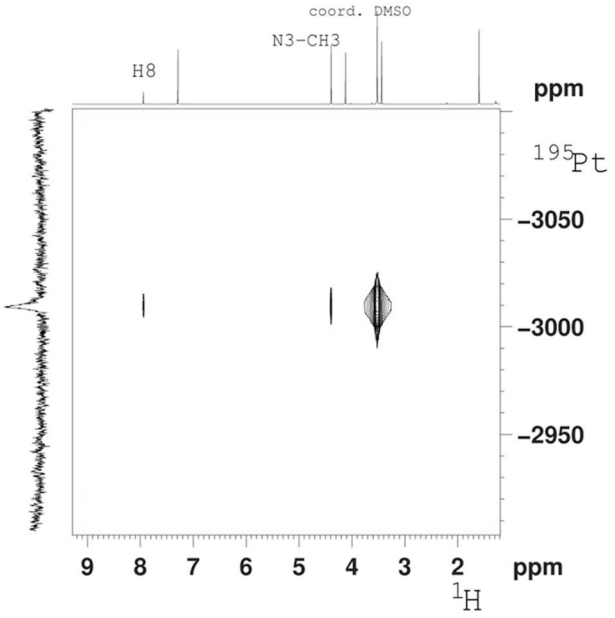

Fig. 1. ^{1}H-^{195}Pt HMQC spectrum of **3** ($CDCl_3$, 298 K). (For interpretation of the references to colour in this figure, the reader is referred to the web version of this article.)

complexes **1** and **2** display a strong decrease of the absorbance at 440 nm, ascribed to the alteration/modification of the original compounds. The caffeine-containing complex **3** is characterized by an initial, slight decrease of its main absorption followed by an increase during the first hour; subsequently, the data obtained up to 24 h do not show any further changes.

Next, the stability of the new Pt complexes was investigated by NMR, which corroborated the results obtained by UV–Vis spectroscopy. The modifications experienced by the complexes in solution after 24 h of incubation are illustrated in Scheme 2. NMR studies indeed confirmed that complexes **1** and **2** were progressively hydrolyzed. In fact, the ^{1}H and $^{13}C\{^{1}H\}$ spectra of a DMSO-d_6 solution of complex **1** left overnight in the NMR tube revealed the presence of free curcumin (half amount with respect to the coordinated ligand). The hydrolysis is significantly faster in the case of complex **2**, which easily loses curcumin during the first hour in solution. In addition, ^{1}H NOESY-EXSY experiments revealed the occurrence of an intense exchange cross-peak between the γ-proton of free curcumin and water (Fig. S3). Furthermore, the ^{1}H-^{195}Pt HMQC spectrum of a sample left 24 h in the NMR tube (containing non-anhydrous solvent) showed the presence of an extra platinum signal at −3446 ppm, correlating to coordinated DMSO methyl protons (Fig. S4). This signal is tentatively assigned to a platinum hydroxy species.

Complex **3** did not undergo hydrolysis. Even after a few days in (non-anhydrous) $CDCl_3$, its NMR spectrum did not show any signals belonging to free caffeine. However, it slowly isomerizes from the *trans* to the *cis* form, leading to an equilibrium mixture. In fact, the ^{1}H-^{195}Pt HMQC spectrum registered after 24 h (Fig. S5) showed the presence of an extra cross-peak at −3457 ppm for ^{195}Pt (correlating with DMSO methyl protons), consistent with a *cis* Pt(II) complex [50]. The ^{1}H and ^{13}C signals of *trans* and *cis* isomers were isochronous [52].

3.3. Photoluminescence properties of curcuminate complexes 1 and 2

Given the emissive nature of curcumin, the photoluminescence spectra of complexes **1** and **2** have been recorded. Fig. 2 displays both the absorbance and the emission spectra of curcumin and complexes **1** and **2** at the same concentration, for comparison. The emission of free curcumin results from its delocalized π-conjugated electronic system, which is strongly influenced by solvents, tautomerism, and structural modifications [53]. Coordination to metal ions may quench the fluorescence through either energy or electron-transfer processes. Namely, square-planar platinum(II) complexes have been shown to exhibit interesting and intriguing photophysical behaviours, associated with the strong tendency to form π-π stacking and Pt···Pt interactions [54].

Curcumin emission (560 nm) is quenched when forming the complexes with platinum(II). Such phenomenon has been observed with other platinum(II) complexes, and is most likely due to the presence of low-lying thermally accessible d–d LF state, which would result in the quenching of the excited state *via* non-radiative decay, totally quenching or diminishing the luminescence. [54] Interestingly, the bis (triphenylphosphane) complex **1** does not only show a stronger quenching of the emission but also a remarkable red shift of the absorbance and emission maxima, with respect to the free curcumin; *i.e.* its absorbance maximum changes from 430 to 470 nm, and its emission shifts from 560 to 660 nm. On the contrary, no shift is observed in the

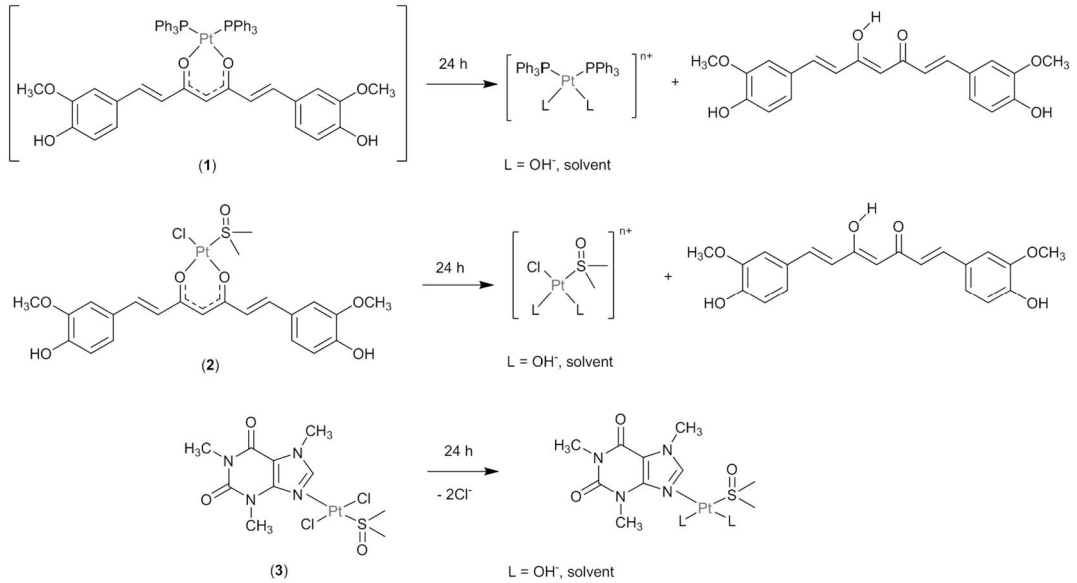

Scheme 2. Hydrolysis of **1** and **2** and isomerization of **3** during 24 h incubation. (For interpretation of the references to colour in this figure, the reader is referred to the web version of this article.)

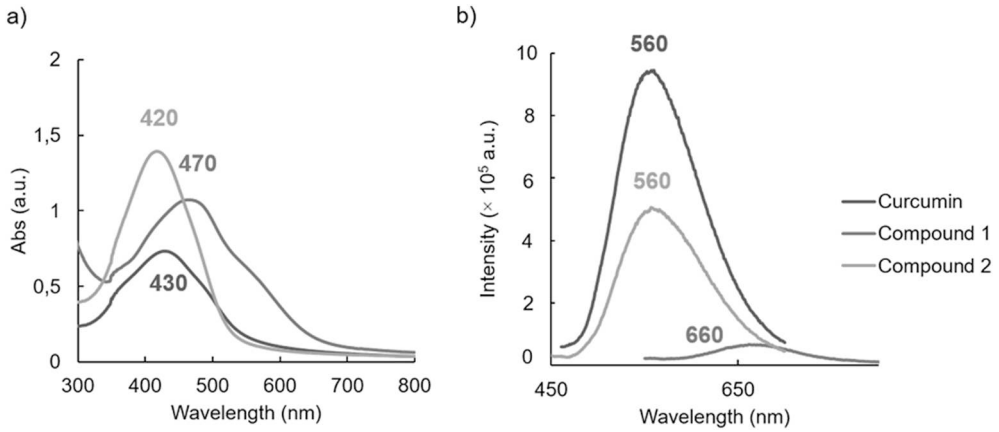

Fig. 2. Absorbance (a) and emission spectra (b) of freshly prepared 30 μM solutions of curcumin and its platinum(II) complexes **1** and **2** in cacodylate-NaCl buffer pH 7.2 (0.3% DMSO). (For interpretation of the references to colour in this figure, the reader is referred to the web version of this article.)

emission maxima of complex **2**.

3.4. DNA-binding studies

DNA is the classical pharmacological target of metal-based anticancer agents; therefore, the *in vitro* study of the interaction of coordination compounds with DNA is of paramount importance to assess the therapeutic potential of the compounds investigated.

The four main ways (but not the only ones) in which small molecules can bind to double-stranded DNA are: (i) intercalation between two adjacent base pairs and perpendicular to the helical axis; (ii) outside-edge binding to the sugar-phosphate backbone of the helix through electrostatic interactions; (iii) groove binding with functional groups into either the major or minor groove and (iv) covalent interaction between DNA and the metal complexes at the nitrogen atoms of nucleobases [55].

Several characterization techniques have been employed to study the interactions of platinum(II) complexes **1**–**3** with DNA, namely UV–Vis spectroscopy, displacement assays of DNA binders, circular dichroism, agarose gel electrophoresis and atomic-force microscopy. It should be stressed that the studies with DNA were carried out using incubation periods of 24 h, during which the complexes hydrolysed (compounds **1** and **2**) and isomerized (compound **3**).

3.4.1. UV–vis spectroscopy

Using increasing amounts of ct-DNA (applying a short incubation time, *viz.* 5 min), the absorption maximum of complex [Pt(curc)$(PPh_3)_2$]Cl (**1**) at 440 nm is shifted towards longer wavelengths, with concomitant decrease of its intensity (Fig. 3c). Such bathochromic and hypochromic effects are generally associated to an intercalative process into the double-stranded DNA. This reduction of the absorption intensity combined with a red shift may arise from strong π - π* stacking interactions between the planar aromatic curcumin ligand and DNA base pairs [56,57]. To take into consideration the hydrolysis of compound **1**, it was also incubated for 24 h (instead of 5 min) with increasing amounts of ct-DNA; however, the precipitation of the modified complex did not allow to carry out this study.

In the case of [PtCl(curc)(DMSO)] (**2**), 5 min-incubation with increasing amounts of ct-DNA, the absorption maximum at 444 nm initially exhibits a hyperchromic effect upon the first addition of DNA, followed by a hypochromic effect in the presence of increasing amounts of the biomolecule, with no wavelength shift (Fig. 3a). These features are consistent with changes of the DNA conformation upon complex binding, either by electrostatic interactions or groove binding [58]. The binding constant (K_b) was calculated applying Eq. 1, giving a value of $8.8 \times 10^5\ M^{-1}$. Hydrolysed **2** (after 24 h incubation with ct-DNA) produced a distinct hypochromic effect (Fig. 3b), which may arise from either electrostatic interactions or groove binding. The [DNA] / ($\varepsilon_a - \varepsilon_f$) *vs.* [DNA] plot reveals the occurrence of two different K_b values, which can be due to the interaction of hydrolysed **2** and free (released) curcumin with the biomolecule [20].

For [Pt(caffeine)Cl_2(DMSO)] (**3**), no changes of the absorption (at $\lambda_{max} = 272$ nm) were observed upon incubation with ct-DNA for 5 min (data not shown). Upon incubation for 24 h, the main absorbance band increased strongly with the first addition of DNA, and only experienced slight changes with more DNA added (Fig. 3d). The observed hyperchromicity indicates a decrease in the degree of parallel stacking in the DNA double helix, which may result from covalent bonding of Pt(II) to purine bases. Similar hyperchromic effects have been reported for cisplatin interacting with DNA, although no batochromism is detected in this case [59]. A high K_b value of $3 \times 10^7\ M^{-1}$ was obtained for **3**.

3.4.2. Displacement assays of fluorescent DNA-binders

To further investigate the nature of the interactions between the platinum(II) complexes **1**–**3** and ct-DNA, competitive binding studies using ethidium bromide (EB) bound to ct-DNA were carried out. EB is a DNA-intercalating agent whose fluorescence emission is nearly 20-fold stronger when bound to the polynucleotide molecule [60,61].

Hence, if a complex is able to displace DNA-bound EB upon interaction with DNA, then a decrease of fluorescence (due to EB release) will be detected. The extent of this displacement can provide information regarding the DNA-binding affinity of the compound considered [62]. It should be stated here that EB displacement does not imply that the interacting compound as an intercalator like EB; electrostatic interactions or groove binding may be sufficient to alter significantly the conformation of the DNA double helix, inducing the release of EB.

Fluorescence spectra of solutions containing constant concentrations (*i.e.* 30 and 75 μM, respectively) of ct-DNA and EB (previously incubated) and increasing amounts of complexes **1**–**3**, *viz.* in the range 0–25 μM, were recorded after 24 h. In all cases, a clear decrease in emission intensity is noticed (Fig. 4). To assess the respective affinity of the different complexes for ct-DNA (compared to EB), their quenching efficiency was evaluated determining the Stern–Volmer quenching constant K_{SV}, applying Eq. (2):

$$\frac{I_0}{I} = 1 + K_{SV}[complex] \quad (2)$$

where I_0 and I are the emission intensities in the absence and the presence of the complex, respectively. Fig. 4 shows the I_0/I values in function of the concentration, for **1**–**3**. The slopes of the corresponding lines gave K_{SV} values of $5.0 \times 10^4\ M^{-1}$, $1.2 \times 10^4\ M^{-1}$, and $7.7 \times 10^3\ M^{-1}$ for **1**, **2** and **3**, respectively. These values reveal moderate EB-displacing abilities, complex [Pt(curc)$(PPh_3)_2$]Cl (**1**) inducing

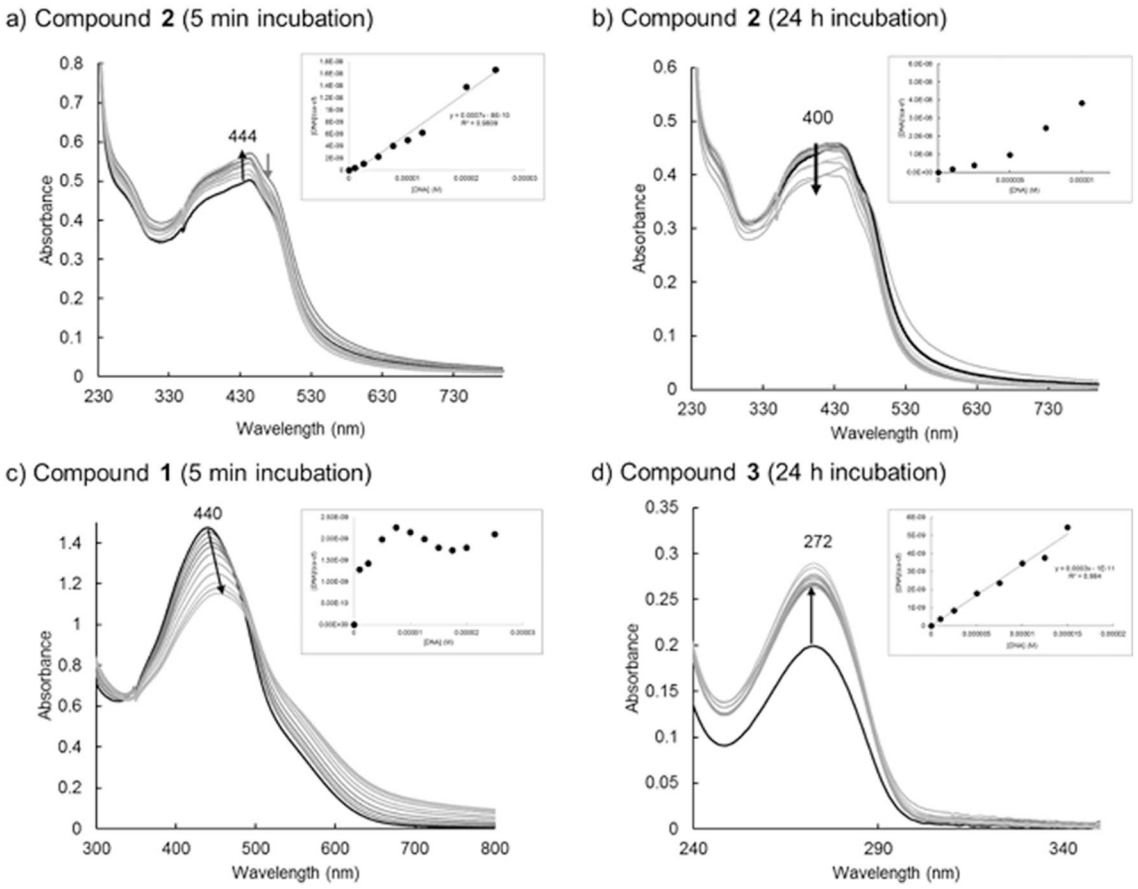

Fig. 3. Absorption spectra of 25 μM solutions of compounds **1–3** without DNA and with increasing amounts of ct-DNA (0–25 μM), in cacodylate buffer (pH = 7.2), at the indicated incubation times (5 min or 24 h). The arrows show the change upon addition of DNA. Insets: Linear fitting of the plots of [DNA] / ($\varepsilon_a - \varepsilon_f$) *vs.* [DNA] for the titration of ct-DNA with complexes **1–3** at the specified wavelengths. (For interpretation of the references to colour in this figure, the reader is referred to the web version of this article.)

a significantly stronger displacement than complexes **2** and **3**. The higher propensity of **1** to act as a possible intercalator (see Section 3.4.1) corroborates the UV–Vis data, which showed a shift of the absorbance maximum for this compound.

Competitive binding studies were next conducted with the minor-groove binder Hoechst 33258. When this dye is bound to ct-DNA, it fluoresces at 458 nm when excited at 350 nm, while its free form emits at 508 nm when excited at 337 nm. As for EB, its fluorescence is dramatically increased upon binding to the biomolecule, over 28-fold as reflected by the corresponding quantum yields [63]. Therefore, displacement of DNA-bound Hoechst 33258 by a metal complex will result in fluorescence quenching if it interacts in the minor groove of the

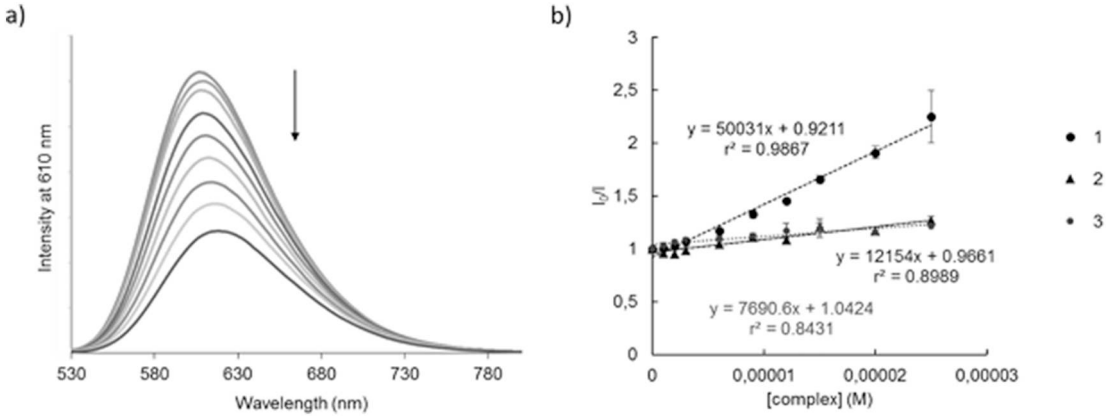

Fig. 4. a) Emission spectra of the DNA–EB complex, upon addition of increasing amounts of compound **1**. The arrow shows the diminution of the emission intensity with the addition of **1**; b) Plots of I_0/I *vs.* complex concentration for the titration of DNA–EB with complexes **1–3**: experimental data points and linear fitting of the data. I_0 corresponds to the maximum emission of the DNA–EB complex in sodium cacodylate buffer (pH = 7.2) and I stands for the maximum emission intensity of the DNA–EB complex after 24 h-incubation with increasing concentrations of complexes **1**, **2** and **3**. [EB] = 75 μM, [DNA] = 30 μM, [complex] = 0–25 μM, λ_{ex} = 514 nm and λ_{em} = 610 nm. Measurements were carried out in duplicate; error bars represent standard deviation values. (For interpretation of the references to colour in this figure, the reader is referred to the web version of this article.)

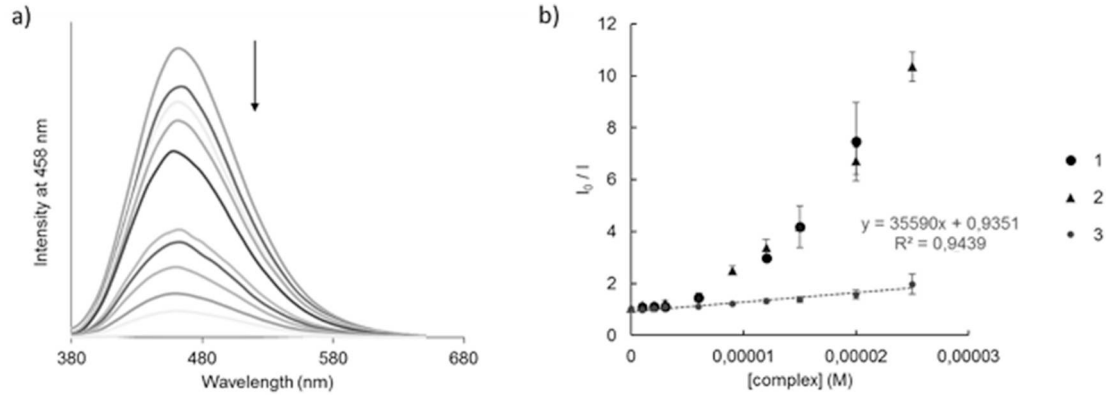

Fig. 5. a) Emission spectra of the DNA–Hoechst33258 complex upon addition of increasing amounts of **2**. The arrow shows the diminution of the emission intensity with the addition of the metal complex; b) Plots of I_0/I *vs.* complex concentration for the titration of Hoechst-DNA with complexes **1–3**: experimental data points and linear fitting of the data. I_0 corresponds to the maximum emission of the Hoechst–DNA complex in sodium cacodylate buffer (pH = 7.2) and I stands for the maximum emission intensity of the Hoechst-DNA after 24 h-incubation with increasing concentrations of complexes **1**, **2** and **3**. [Hoechst33258] = 100 μM, [DNA] = 30 μM, [Complex] = 0–25 μM, λ_{ex} = 350 and λ_{em} = 458 nm. Measurements were carried out in duplicate; error bars represent standard deviation values. (For interpretation of the references to colour in this figure, the reader is referred to the web version of this article.)

double helix.

Increasing amounts of complexes **1–3** were added to ct-DNA (30 μM, in terms of nucleobases) and Hoechst 33258 (100 μM). In all cases, the emission of the Hoechst-DNA complex gradually decreased upon complex addition (see Fig. 5a for compound **2**). The fluorescence decrease was not linear for the bulkier curcumin complexes **1** and **2** at concentrations above 3 μM, as observed in Fig. 5b. Such a non-linear quenching phenomenon may be attributed to an energy-transfer process between the dye and the released curcumin from complexes **1** and **2**; it can indeed be noted that the emission of the dye (λ_{em} = 458 nm) and the absorbance of free curcumin (λ_{max} = 430 nm; Fig. 2a) overlap. Hence, the extent of dye displacement and the energy-transfer contribution could not be discerned for any of these complexes. A weak groove binding of free curcumin should also not be ignored in this displacement assay. [20]

Therefore, the Stern-Volmer Eq. (2) could only be applied to **3**, which gave a K_{SV} value of $3.6 \times 10^4\ M^{-1}$. This K_{SV} value, obtained with the groove-binder Hoechst 33258, is five times higher than achieved by competitive binding with the intercalator EB. Such an effect may be caused by the kinking of the DNA double helix through cis-bidentate, covalent binding, which is suggested as well by the UV–Vis data.

From the relatively low K_{SV} value obtained for **2** in the EB displacement assays, it can be considered that it is not acting as intercalator either; most likely, it interacts with ct-DNA electrostatically or *via* groove binding.

3.4.3. Circular dichroism (CD)

The CD spectrum of natural calf thymus DNA consists of a positive band at 275 nm due to base stacking and a negative band at 245 nm due to the characteristic helicity of the right-handed B form. The effect of **1–3** on the secondary structure of ct-DNA was studied with a constant concentration of DNA by increasing the complex concentration up to one equivalent with respect to the concentration of nucleobases, except for complex **1**, which precipitated at complex:DNA ratios over 0.2 (Fig. 6).

In the presence of **1**, the intensity of the positive peak increased, and the intensity of the negative peak decreased. This phenomenon was accompanied by a hypsochromic shift of both peaks. These observations are consistent with an intercalative process [64].

The incubation of ct-DNA with complexes **2** and **3** gave rise to a decrease of the intensity of both the positive and negative signals, accompanied by a bathochromic shift. These changes are indicative of alterations of the secondary structure of B-DNA, probably as a result of a non-intercalative interaction of the complexes with the double helix.

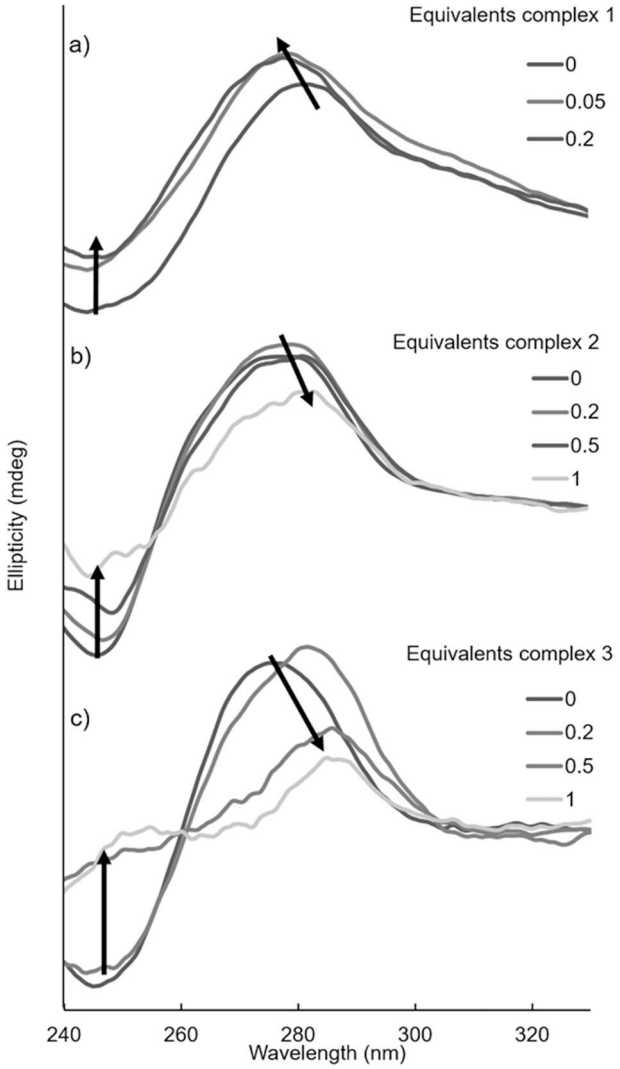

Fig. 6. Circular dichroism spectra of ct-DNA (200 μM) in the presence of increasing amounts of complexes **1** (a), **2** (b) and **3** (c), in 1.0 mM cacodylate – 20 mM NaCl buffer (pH = 7.2). The spectra were recorded after 24 h incubation at 37 °C. Precipitation was observed for **1** at complex:DNA ratios above 0.2. (For interpretation of the references to colour in this figure, the reader is referred to the web version of this article.)

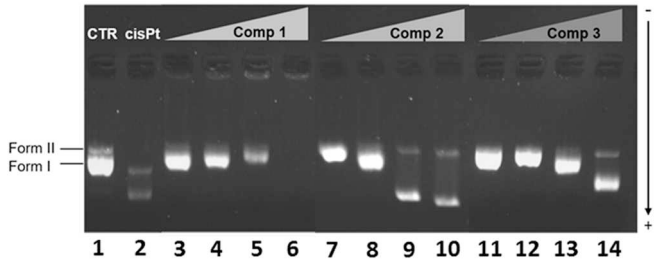

Fig. 7. Agarose gel electrophoresis images of pBR322 plasmid DNA (50 μM base pairs) incubated for 24 h at 37 °C with increasing concentrations of the different complexes in cacodylate-NaCl buffer pH 7.2. Lanes 1 and 2 contain non-treated DNA and DNA treated with 10 μM cisplatin. The other lanes correspond to increasing concentrations, namely 5, 10, 25 and 50 μM, of compounds **1** (lanes 3–6), **2** (lanes 7–10) and **3** (lanes 11–14). (For interpretation of the references to colour in this figure, the reader is referred to the web version of this article.)

The effect was remarkably stronger for **3** and is comparable to that observed for cisplatin, *i.e. cis*-[$PtCl_2(NH_3)_2$]; these features suggest a cis-bidentate covalent binding of **3** to DNA, which is consistent with the UV–Vis measurements and allowed by a *trans*-to-*cis* isomerization upon incubation of the compounds [65].

Finally, it can be pointed out that, at the complex concentrations used, induced CD signals in the metal-to-ligand charge transfer region were not detected.

3.4.4. Agarose gel electrophoresis

The interaction of the Pt(II) complexes with DNA can be visualized by agarose gel electrophoresis through the changes they produce to the DNA conformation. These structural changes are reflected by distinct electrophoretic mobilities. pBR322 DNA usually presents about 90% of supercoiled form (Form I) and 10% of the nicked form (Form II). The most intense band of the non-treated DNA sample in Fig. 7, lane 1 corresponds to form I (supercoiled DNA), which migrates faster than form II (nicked or relaxed circular DNA); being more compact, form I is less retained in the gel. Fig. 7 also shows the effects of increasing concentrations of complexes **1–3** (from 5 to 50 μM) on the DNA structure, after incubation of 24 h.

A slight decrease of the electrophoretic mobility of DNA is observed with increasing amounts of **1** (Fig. 7, lanes 3–6), which results from the unwinding of the double helix due to the intercalation of the complex. The bands gradually lose their intensity, suggesting that the DNA is cleaved into undetectable single-stranded pieces; the intermediate linear form III is not detected. Since the samples were exposed to daylight during their preparation (except during the incubation step), the observed degradation may result from photocleavage, a feature that has been reported for other platinum(II) complexes containing curcumin, which has a photosensitizing character [28]. The oxidative photo-induced damage of **1** may be favoured by its intercalation between nucleobase pairs; this would also explain why such a damage is not observed for the other curcumin-containing compound **2**.

The behaviour of **2** displays is similar to that of the caffeine-containing complex **3**. At low concentrations of these two complexes, the respective bands observed (Fig. 7, lanes 7–8 and 11–12, respectively) suggest an unwinding of the supercoiled form, leading to the coalescence of form I and II. At higher concentrations, namely 25 and 50 μM, complexes **2** and **3** produce a gradual shrinking of the relaxed circular form and, more especially, of the supercoiled form (Fig. 7, lanes 9–10 and 13–14, respectively); this effect results in a higher electrophoretic mobility. These data are consistent with a non-intercalative interaction of the compounds with the biomolecule. It can be pointed out that the effect is more pronounced for **2**.

3.4.5. AFM analysis

Atomic force microscopy (AFM) investigations were carried out with pBR322 plasmid DNA incubated at 37 °C in the dark for 24 h with complexes **2** and **3**. The effect of **1** could not be examined with this technique because it co-precipitated with DNA at the concentrations used for these studies.

The AFM images presented in Fig. 8 show the open circular form of plasmid DNA with some degree of supercoiling (as observed by electrophoresis), and their subsequent morphological alteration upon incubation with different concentrations of compounds **2** and **3**. Fig. 8b and c clearly illustrate that the incubation of DNA with **2** caused a marked shrinking (supercoiling) of the biomolecule, generating small aggregates with a nearly globular shape, especially at higher complex concentrations. A similar but less pronounced effect could be observed for **3** (Fig. 8d and e). The drastic morphological changes noticed are consistent with the gel electrophoresis results.

3.5. In vitro cytotoxic activity

First, single-point cell-viability assays (MTT) were carried out with the free ligands (curcumin and caffeine) and their complexes **1–3** at two concentrations, namely 10 μM and 50 μM (except for **1**), using five cancer cell lines, namely A549 (lung adenocarcinoma), A375 (melanoma), MCF-7 (breast adenocarcinoma), SKOV3 (ovary adenocarcinoma) and SW620 (colorectal adenocarcinoma). The results obtained upon incubating the freshly prepared solutions of the compounds with the cells during 24 h are depicted in Fig. S6. Compounds [Pt(curc)$(PPh_3)_2$]Cl (**1**) and [PtCl(curc)(DMSO)] (**2**) exhibited the best activities, particularly against SW620 and MCF-7 cells. It should be noted that the extremely low aqueous solubility of the curcumin-based complex **1** did not allow testing it at 50 μM, where visible aggregates formed in the wells. Neither caffeine nor its complex *trans*-[Pt(caffeine)Cl_2(DMSO)] (**3**) showed significant toxicity against the selected cell lines.

Next, dose-response curves and the corresponding IC_{50} values were produced for the cancer cell lines SW620 and MCF-7, and the non-tumorigenic cell line MCF-10A to assess the potential selectivity of the compounds towards malignant cells (Table 1). Because of the above-mentioned low aqueous solubility of compound **1**, the corresponding IC_{50} at%DMSO below cell tolerance could not be obtained.

Since the described compounds herein are inspired by cisplatin, this drug has been selected as reference for these studies. Cisplatin showed remarkably different cytotoxicities depending on whether its stock solution was prepared in DMSO or in PBS. The higher stability of the complex *cis*-[$Pt(DMSO)_2(NH_3)_2$], which results from the replacement of the chlorido ligands of cisplatin by the softer S-ligand DMSO, most likely is responsible for its inertness and consequent lack of cytotoxicity (IC_{50} > 100 μM). In fact, cisplatin dissolved in DMSO was nontoxic for all the cell lines tested (maximum concentration used 100 μM, data not shown), whereas cisplatin dissolved in PBS reduced the cell viability at lower doses (IC_{50} ranging from 12 to 28 μM).

The nontoxic nature of DMSO-dissolved cisplatin is in sharp contrast with the high toxicity of the Pt(II) complexes **1** and **2**, which were also (and necessarily) dissolved in DMSO prior to their addition to the cell media. Curcumin and its complex **2** showed interesting antiproliferative activities and revealed a clear enhancement of the activity upon metal complexation; for instance, compound **2** exhibited an IC_{50} value as low as 6.1 μM against SW620 cells while the IC_{50} of free curcumin was 15.5 μM. With MCF-7 cells, the toxicity increase was even higher upon metal complexation. To assess the effect of the hydrolysed form of **2** in combination with the released curcumin, the compounds were pre-incubated for 24 h in the cell media before IC_{50} determination. The resulting toxicity was significantly lower in all cell lines for both curcumin and the hydrolysis products of **2**. This observation may be due to the sequestration/binding of the hydrolysed platinum(II) compound (see Scheme 2) and the free curcumin by the serum proteins present in the cell media; curcumin can interact with serum albumins through the hydroxyl phenolic groups, [66] and the aquated form(s) of platinum(II) complex **2** may bind covalently with protein thiols. Similarly, the

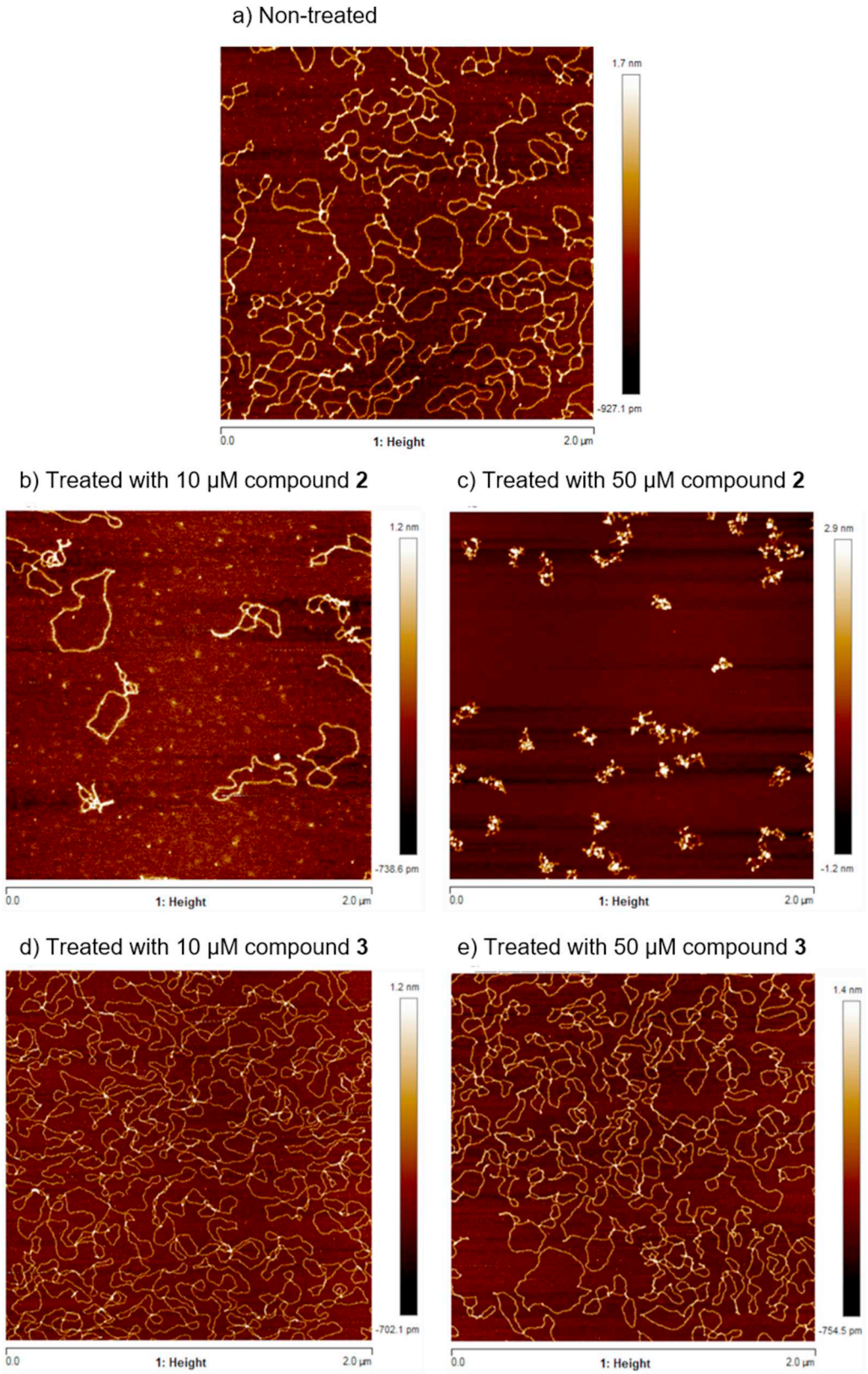

Fig. 8. AFM micrographs of plasmidic pBR322 DNA incubated for 24 h (a) without complex and in the presence of (b) 10 µM **2**, (c) 50 µM **2**, (d) 10 µM **3** and (e) 50 µM **3**. $[DNA]_{bp} = 15$ µM.

cytotoxic effect of cisplatin was reduced when it was pre-incubated in the cell media (> 85% cell viability at 20 µM).

Next, we evaluated the effect of the photosensitizing nature of curcumin and its complexes on their cytotoxicity against SW620 and MCF-7 cells, and the non-tumorigenic cells MCF-10A. Curcumin reaches a triplet state upon photoactivation with visible light (strong absorption centred at 430 nm), and it reacts with molecular oxygen to generate reactive oxygen species (ROS) [28]. The irradiation of free curcumin

and compound **2** (both freshly prepared and pre-incubated) with visible light for 1 h increased their toxicity (Table 1). According to the IC_{50} values obtained, the photosensitization was generally higher for free curcumin than for **2**. In line with this observation, the photosensitizing effect was also more significant for the hydrolysed forms of the compounds. The smaller differences observed with SW620 cells upon irradiation may be attributed to the higher amounts of the ROS-scavenger cysteine contained in the culture media used (for this cell line). Expectedly, the irradiation of cisplatin with visible light did not improve its toxicity.

In all cases (namely with or without pre-incubation and with or without visible-light irradiation), [PtCl(curc)(DMSO)] (**2**) displayed similar or higher cytotoxicities than its parent compound, *viz.* cisplatin. Furthermore, the freshly prepared solution of **2** showed better selectivity towards cancer cells than both curcumin and cisplatin.

4. Conclusions

Three new Pt(II) complexes, containing curcuminate, *viz.* [Pt(curc)$(PPh_3)_2$]Cl (**1**) and [PtCl(curc)(DMSO)] (**2**), or caffeine, *viz. trans*-[Pt(caffeine)Cl_2(DMSO)] (**3**), were synthesized and characterized. The curcuminate ligands coordinate through its β-diketonate moiety, while caffeine binds Pt through its N^9 atom. A thorough study of their interaction with DNA through a range of spectroscopic techniques, AFM and gel electrophoresis, revealed distinct behaviours for the different compounds. Complex **1** tends to intercalate in between nucleobase pairs while for complex **2**, which contains a chloride and DMSO ligands instead of PPh_3, the binding seems to occur in the grooves, predominantly driven by electrostatic forces at high compound:DNA molar ratios. Complex **3** appears to interact by covalent bonding with DNA nucleobases, in a cisplatin-like fashion. The three complexes underwent important changes during the first 24 h in solution, and this fact determined their interaction with DNA; this observation has been nicely illustrated in the case of **3**. Speciation studies are required to determine the nature of the species generated.

In addition, the cytotoxic activity of these Pt(II) compounds has been evaluated *in vitro* against five cancer cell lines (A549, A375, MCF-7, SKOV3 and SW620) and one normal breast cell line (MCF-10A) to assess their selectivity. The curcuminate complexes **1** and **2** were rather cytotoxic after 24 h incubation with the cells, while the caffeine complex **3** was not. Remarkably, the curcuminate complex **2** exhibited IC_{50} values in the low micromolar range. The curcuminate moiety allowed the photosensitization of this complex, producing an even more efficient system. This “combined” compound surpassed its parent drugs cisplatin and curcumin, both in toxicity and selectivity. The pre-incubation of all compounds in the cell media lowered their efficacy, which is ascribed to their sequestration by the serum proteins. This observation highlights the importance of including pre-incubation tests in routine cell-viability studies in order to better assess their potential therapeutic use.

The data achieved in the present study clearly illustrate the high potential of curcumin-based metal complexes for possible applications in anticancer drug design.

Acknowledgements

The authors gratefully acknowledge financial support from Ministerio de Ciencia, Innovación y Universidades (MICINN project CTQ2017-88446-R AEI/FEDER, UE) and from Italian Ministero dell'Istruzione dell'Università e della Ricerca (MIUR PRIN project 2010–2011 n. 2010FPTBSH, NANOMED) and from Instituto de Salud Carlos III (ISCIIIFIS PI18/00441, FEDER). A.B.C. acknowledges the European Union's Horizon 2020 research and innovation programme for her Marie Skolodowska-Curie grant No. 656820. P.G. acknowledges the Institució Catalana de Recerca i Estudis Avançats (ICREA). P.M. thanks Dr. Hamid Reza Shahsavari for useful discussions. MPH acknowledges Fundación la Caixa for her postdoctoral fellowship.

Appendix A. Supplementary data

Supplementary data to this article can be found online at https://doi.org/10.1016/j.jinorgbio.2019.110749.

References

[1] J. Ferlay, I. Soerjomataram, M. Ervik, R. Dikshit, S. Eser, C. Mathers, M. Rebelo, D. M. Parkin, D. Forman, F. Bray, vol. 2017, International Agency for Research on Cancer, Lyon, France, 2013.
[2] F. Bray, A. Jemal, N. Grey, J. Ferlay, D. Forman, Lancet Oncol 13 (2012) 790–801.
[3] R.F. Brissos, L. Korrodi-Gregório, R. Péres-Tomás, O. Roubeau, P. Gamez, Chem. Sq. 2 (2018) 4.
[4] J.-A. Cuello-Garibo, C.C. James, M.A. Siegler, S. Bonnet, Chem. Sq 1 (2017) 2.
[5] A. Presa, G. Vazquez, L.A. Barrios, O. Roubeau, L. Korrodi-Gregorio, R. Perez-Tomas, P. Gamez, Inorg. Chem. 57 (2018) 4009–4022.
[6] J.M. Saborit, A. Caubet, R.F. Brissos, L. Korrodi-Gregorio, R. Perez-Tomas, M. Martinez, P. Gamez, Dalton Trans. 46 (2017) 11214–11222.
[7] B. Rosenberg, L. VanCamp, J.E. Trosko, V.H. Mansour, Nature 222 (1969) 385–386.
[8] F. Arnesano, G. Natile, Coord. Chem. Rev. 253 (2009) 2070–2081.
[9] B.A. Chabner, T.G. Roberts Jr., Nat. Rev. Cancer 5 (2005) 65–72.
[10] C.A. Rabik, M.E. Dolan, Cancer Treat. Rev. 33 (2007) 9–23.
[11] R.P. Miller, R.K. Tadagavadi, G. Ramesh, W.B. Reeves, Toxins 2 (2010) 2490–2518.
[12] F.E. de Jongh, R.N. van Veen, S.J. Veltman, R. de Wit, M.E. van der Burg, M.J. van den Bent, A.S. Planting, W.J. Graveland, G. Stoter, J. Verweij, Br. J. Cancer 88 (2003) 1199–1206.
[13] C. Monneret, Ann. Pharm. Fr. 69 (2011) 286–295.
[14] G. Momekov, D. Momekova, Expert Opin Ther Pat 16 (2006) 1383–1403.
[15] T. Boulikas, M. Vougiouka, Oncol. Rep. 10 (2003) 1663–1682.
[16] T.C. Johnstone, K. Suntharalingam, S.J. Lippard, Chem. Rev. 116 (2016) 3436–3486.
[17] S. Wanninger, V. Lorenz, A. Subhan, F.T. Edelmann, Chem. Soc. Rev. 44 (2015) 4986–5002.
[18] M. Pröhl, U.S. Schubert, W. Weigand, M. Gottschaldt, Coord. Chem. Rev. 307 (2016) 32–41.
[19] U. Ndagi, N. Mhlongo, M.E. Soliman, Drug Des Devel Ther 11 (2017) 599–616.
[20] S. Nafisi, M. Adelzadeh, Z. Norouzi, M.N. Sarbolouki, DNA Cell Biol. 28 (2009) 201–208.
[21] M. Heger, R.F. van Golen, M. Broekgaarden, M.C. Michel, Pharmacol. Rev. 66 (2014) 222–307.
[22] Y. Sunagawa, Y. Katanasaka, K. Hasegawa, T. Morimoto, PharmaNutrition 3 (2015) 131–135.
[23] S. Prasad, A.K. Tyagi, B.B. Aggarwal, Cancer Res. Treat. 46 (2014) 2–18.
[24] Y. Kawano, M. Nagata, T. Kohno, A. Ichimiya, T. Iwakiri, M. Okumura, K. Arimori, Biol. Pharm. Bull. 35 (2012) 400–407.
[25] B. Bertrand, L. Stefan, M. Pirrotta, D. Monchaud, E. Bodio, P. Richard, P. Le Gendre, E. Warmerdam, M.H. de Jager, G.M. Groothuis, M. Picquet, A. Casini, Inorg. Chem. 53 (2014) 2296–2303.
[26] Y. Oda, M. Hidaka, A. Suzuki, Biol. Pharm. Bull. 40 (2017) 2005–2009.
[27] A.K. Renfrew, N.S. Bryce, T.W. Hambley, Chem. Sci. 4 (2013) 3731.
[28] K. Mitra, S. Gautam, P. Kondaiah, A.R. Chakravarty, Angew Chem Int Ed Engl 54 (2015) 13989–13993.
[29] F.R. Hartley, The Chemistry of Platinum and Palladium: With Particular Reference to Complexes of the Elements, Applied Science Publishers, 1973.
[30] Y.Yu.N. Kukushkin, E. Vyaz'menskii, L.I. Zorina, Russ. J. Inorg. Chem. 13 (1968) 1573–1576.
[31] K. Nakamoto, M. Tsuboi, G.D. Strahan, Methods Biochem. Anal. 51 (2008) 1–366.
[32] K.I. Priyadarsini, Molecules 19 (2014) 20091–20112.
[33] P. Bergamini, V. Ferretti, P. Formaglio, A. Marchi, L. Marvelli, F. Sforza, Polyhedron 78 (2014) 54–61.
[34] A. Medrano, S.M. Dennis, A. Alvarez-Valdes, J. Perles, T. McGregor Mason, A.G. Quiroga, Dalton Trans. 44 (2015) 3557–3562.
[35] M.M. Dell'Anna, V. Censi, B. Carrozzini, R. Caliandro, N. Denora, M. Franco, D. Veclani, A. Melchior, M. Tolazzi, P. Mastrorilli, J. Inorg. Biochem. 163 (2016) 346–361.
[36] M. Ravera, E. Gabano, M. Sardi, E. Monti, M.B. Gariboldi, D. Osella, Eur. J. Inorg. Chem. (2012) 3441–3448.
[37] D.G. Gusev, Angew Chem Int Ed Engl 51 (2012) 12930–12931.
[38] R. Benassi, E. Ferrari, S. Lazzari, F. Spagnolo, M. Saladini, J. Mol. Struct. 892 (2008) 168–176.
[39] M.S. Refat, Spectrochim. Acta A 105 (2013) 326–337.
[40] F. Kühlwein, K. Polborn, W. Beck, Z. Anorg. Allg. Chem. 623 (1997) 1211–1219.
[41] F. Kühlwein, K. Polborn, W. Beck, Z. Anorg. Allg. Chem. 623 (1997) 1931–1944.
[42] K. Nakamoto, Handbook of Vibrational Spectroscopy, Major Reference Works, (2001).
[43] M.M. Dell'Anna, U. Englert, M. Latronico, P.L. Luis, P. Mastrorilli, D.G. Papa, C.F. Nobile, M. Peruzzini, Inorg. Chem. 45 (2006) 6892–6900.
[44] J. do Couto Almeida, I.M. Marzano, F.C.S. de Paula, M. Pivatto, N.P. Lopes, P.C. de Souza, F.R. Pavan, A.L.B. Formiga, E.C. Pereira-Maia, W. Guerra, J. Mol. Struct. 1075 (2014) 370–376.
[45] S.A. De Pascali, P. Papadia, A. Ciccarese, C. Pacifico, F.P. Fanizzi, Eur. J. Inorg. Chem. (2005) 788–796.
[46] M. Melnik, O. Sprusansky, P. Musil, Adv Biol Chem 4 (2014) 274–280.
[47] N. Raman, K. Pothiraj, T. Baskaran, J. Mol. Struct. 1000 (2011) 135–144.

[48] N. Shahabadi, N. Moeini, J. Coord. Chem. 68 (2015) 2871–2885.
[49] C. Sacht, M.S. Datt, S. Otto, A. Roodt, J. Chem. Soc. Dalton Trans. (2000) 727–733.
[50] L.G. Marzilli, Y. Hayden, M.D. Reily, Inorg. Chem. 25 (1986) 974–978.
[51] J. Sitkowski, L. Stefaniak, L. Nicol, M.L. Martin, G.J. Martin, G.A. Webb, Spectrochim. Acta A 51 (1995) 839–841.
[52] I. Łakomska, B. Golankiewicz, J. Wietrzyk, M. Pełczyńska, A. Nasulewicz, A. Opolski, J. Sitkowski, L. Kozerski, E. Szłyk, Inorg. Chim. Acta 358 (2005) 1911–1917.
[53] R. Ghosh, J.A. Mondal, D.K. Palit, J. Phys. Chem. B 114 (2010) 12129–12143.
[54] V.W. Yam, K.M. Wong, Chem. Commun. 47 (2011) 11579–11592.
[55] M.J. Hannon, Pure Appl. Chem. 79 (2007) 2243–2261.
[56] J.M. Kelly, A.B. Tossi, D.J. McConnell, C. OhUigin, Nucleic Acids Res. 13 (1985) 6017–6034.
[57] S.U. Rehman, T. Sarwar, M.A. Husain, H.M. Ishqi, M. Tabish, Arch. Biochem. Biophys. 576 (2015) 49–60.
[58] M. Sirajuddin, S. Ali, A. Badshah, J. Photochem. Photobiol. B 124 (2013) 1–19.
[59] Y. Zou, L. Biao, F. Xu, R. Liu, Z. Liu, Y. Fu, Scanning 38 (2016) 880–888.
[60] J.B. LePecq, C. Paoletti, J. Mol. Biol. 27 (1967) 87–106.
[61] F.J. Meyer-Almes, D. Porschke, Biochemistry 32 (1993) 4246–4253.
[62] R.F. Brissos, E. Torrents, F.M. dos Santos Mello, W. Carvalho Pires, P. Silveira-Lacerda Ede, A.B. Caballero, A. Caubet, C. Massera, O. Roubeau, S.J. Teat, P. Gamez, Metallomics 6 (2014) 1853–1868.
[63] G. Cosa, K.S. Focsaneanu, J.R. McLean, J.P. McNamee, J.C. Scaiano, Photochem. Photobiol. 73 (2001) 585–599.
[64] N. Shahabadi, N.H. Moghadam, Spectrochim. Acta A 99 (2012) 18–22.
[65] J.-P. Macquet, J.-L. Butour, Eur. J. Biochem. 83 (1978) 375–387.
[66] F. Mohammadi, A.K. Bordbar, A. Divsalar, K. Mohammadi, A.A. Saboury, Protein J. 28 (2009) 189–196.